

## LA-UR-19-30924

Approved for public release; distribution is unlimited.

Title: Study of Neutron-Induced Stable and Radioactive Nuclides in a Post  
Detonation Urban Environment

Author(s): McClanahan, Tucker Caden

Intended for: Report

Issued: 2019-10-28

---

**Disclaimer:**

Los Alamos National Laboratory, an affirmative action/equal opportunity employer, is operated by Triad National Security, LLC for the National Nuclear Security Administration of U.S. Department of Energy under contract 89233218CNA000001. By approving this article, the publisher recognizes that the U.S. Government retains nonexclusive, royalty-free license to publish or reproduce the published form of this contribution, or to allow others to do so, for U.S. Government purposes. Los Alamos National Laboratory requests that the publisher identify this article as work performed under the auspices of the U.S. Department of Energy. Los Alamos National Laboratory strongly supports academic freedom and a researcher's right to publish; as an institution, however, the Laboratory does not endorse the viewpoint of a publication or guarantee its technical correctness.

# Study of Neutron-Induced Stable and Radioactive Nuclides in a Post Detonation Urban Environment

Tucker C. McClanahan

September 25, 2019

## 1 Introduction

In the event of a nuclear detonation in an urban environment, response time for triage by first responders, and forensic sample collection are of the utmost importance. When it comes to response planning, decision makers within the government need to have the most up-to-date information regarding several quantities of interest so that the maximum amount of lives can be saved. Quantities of interest in a post-detonation scenario include the spatial distribution of neutron-induced stable and radioactive isotopes in the environment, fallout patterns, blast and fire damage zones [1]. The UMPRINDER toolkit is developed to calculate the prompt neutron-induced stable and radioactive isotopes in the surrounding environment in a nuclear forensics post-detonation scenario. The distribution of these isotopes in the environment can be used to provide guidance in determining best routes for first responders in order to minimize dose, debris sample collection routes for subsequent radiochemical analysis, and provide initial radionuclide inventories to fallout codes in order to improve fallout zone fidelity. Other methods have approached isotope transmutation on unstructured mesh for the fusion community concerning shutdown dose rates associated with fusion reactors. UMPRINDER is the first method to be focused on calculating some of the quantities of interest for the nuclear forensics and weapon effects communities.

## 2 Methods

The UMPRINDER toolkit includes two main modules: the Material Processing module (Section 2.1) and the Activation module (Section 2.2). The Material Processing module pulls from various material composition databases and publications to provide homogenized materials for the initial MCNP6.2 run. The Activation module couples MCNP6.2 and latest release of CINDER2008 as apart of the AARE package using a Python wrapper to translate the fluxes on the unstructured mesh geometry from the initial MCNP6.2 run into input files for CINDER2008. The Activation module then executes individual CINDER2008 runs in parallel using OpenMP or MPI, and post-processes the outputs from the CINDER2008 runs for direct analysis.

### 2.1 Overview of the Material Processing Module

The Material Processing module is included with the toolkit to help set up the original MCNP6.2 run with materials often found in an urban environment: soil composition based on latitude and longitude interpolated from USGS data, building construction materials separated by building type, homogenized materials of the building interior based on building type, and homogenized materials of various electronics, e.g. laptops, cellphones, hard disks, etc [2].

Table 1 tabulates a summary of the electronic, structural, and soil materials that are included in the Material Processing Module along with a short description of the origin of the material composition.

The USGS Series 801 data is linearly interpolated between the sample locations using SciPy's `interpolate.griddata` function for the location of interest for the user [3]. The output of the terrain processing portion of the Material Processing Module is three MCNP6 material cards detailing the PPM level elemental composition of the soil for the three USGS categories of soil: Top 5 cm, A horizon (5-10 cm), and C horizon (80-100 cm). Figure 1 illustrates the Quartz wt % at sample locations across the United States that are included in the USGS Series 801 data. The density of the interpolated soil composition is  $1.52 \text{ g/cm}^3$  based on generic soil from PNNL's report.

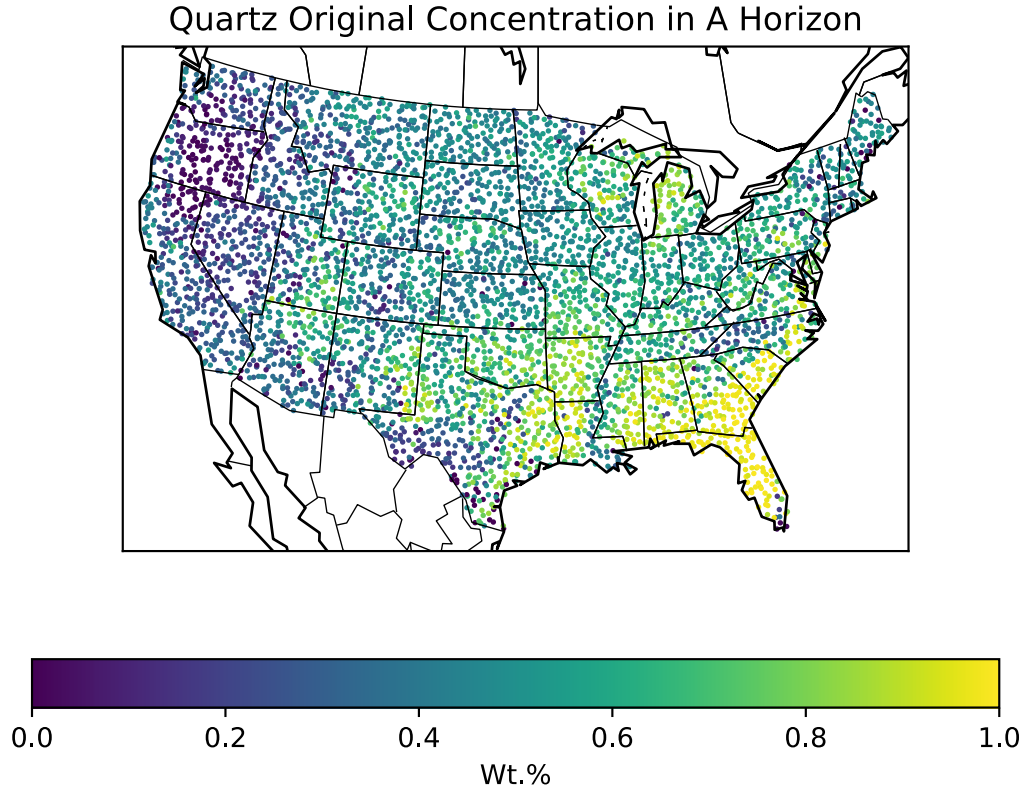


Figure 1: Example of the raw data from USGS Series 801 [2]

In order to properly represent a homogeneous building, the relative abundances of structural materials were incorporated into the Material Processing Module from Kleeman and colleagues' studies that characterize the gross composition of buildings for demolition purposes [4,5]. Building categories from Kleeman and colleagues are applied to the city models based on building size and rough building type determined by the city building code.



Table 1

Material Processing Data Summary Table (PPM= parts per million, MA= most abundant)			
Name	Density (g/cm <sup>3</sup> )	Level of Detail	Reference
Notebook Computer	1.42	PPM	Figure 2 [6] and Table 1 [7]
Lithium Ion Battery	1.73	PPM	Table 2 [8]
Hard Drive Disk	2.37	PPM	Figures 4 & 7 [6]
NdFeB Magnets	7.5	PPM	Table 2 [6]
PCB	1.85	PPM	Table 1 PCB-1 [9]
Mobile Phone	2.177	PPM	Table 4 Average [8]
Carbon Steel	7.82	MA	[10]
Dry Air	0.001205	MA	[10]
Suburban Air	0.001205	PPM	Table 7 Average [11]
Fired Brick	2.1	MA	[10]
PPM Fired Brick	2.1	PPM	[12]
Southern Pine Wood	0.64	MA	[10]
Average Northern Wood	0.64	PPM	Table 3 Spruce [13] Table 5 Mean [14]
Spruce Wood	0.45	PPM	Tables 2 & 3 [13] & Table 1 [15]
Fir Wood	0.51	PPM	Tables 2 & 3 [13]
NIST SRM 612 Glass	2.4	PPM	[16]
Plate Glass	2.4	PPM	MA [10] and PPM [17]
Fly Ash Concrete	1.83	PPM	MF30 Table 1 [18] and Table S7 [19]
Silica Fume Concrete	2.02	PPM	MS10 Table 1 [18]
Blast Furnace Slag Concrete	1.89	PPM	MB30 Table 1 [18]
Quartz	NA	MA	[20]
Kaolin	NA	MA	[21]
Chlorite	NA	MA	[21]
Sepiolite	NA	MA	[21]
Calcite	NA	MA	[20]
Gibbsite	NA	MA	[20]
Dolomite	NA	MA	[22]
Aragonite	NA	MA	[23]
Zeolite	NA	MA	[24]
Gypsum	NA	MA	[20]
Talc	NA	MA	[20]
Hornblende	NA	MA	[25]
Serpentine	NA	MA	[20]
Hematite	NA	MA	[20]
Goethite	NA	MA	[20]
Pyroxene	NA	MA	[2]
K Feldspar	NA	MA	[2]
Plagioclase Feldspar	NA	MA	[2]
Pyrite	NA	MA	[2]

## 2.2 Overview of the Activation Module

The Activation Module implements a solution strategy similar to the rigorous 2-step (R2S) system with the exception that the end goal is an isotopic inventory for each mesh element for subsequent analysis [26]. The Activation Module allows the user to calculate the isotopic inventory for each mesh element in the model, and when all of the processes have finished the transmutation runs, it produces a HDF5 database coupled with a XDMF file for direct viewing of results in ParaView or VisIT [27–30].

The Activation Module initializes the transmutation calculation by loading in the material definitions from the MCNP6.2 output file, elemental fluxes on the MCNP6.2 EEOUT file, and isotopic natural abundances and other elemental data from the CINDER2008 BIGZA file. The Activation Module translates the MCNP6.2 material definitions into CINDER2008 material definitions by breaking up the element definitions, if present, into their natural isotopics and assigning each nuclide their own atom fractions. If specific isotopes are specified, the code directly translates the atom fractions from the MCNP6.2 material definitions to CINDER2008 material definitions. Fluxes from the EEOUT file are linearly interpolated to match the cinder cross section energy group structure. The user is free to choose any arbitrary energy bin structure when binning the fluxes in MCNP6.2 but in order to minimize interpolation error, the MCNP6.2 energy bin structure should be the same as the cinder cross section library used in the transmutation calculation. The Activation Module fully automates the production of the CINDER2008 input files and parallelizes the transmutation calculations by executing CINDER2008 on several processes.

Once the transmutation calculation has been initialized, the parallelization scheme is set up depending on whether the user elects to use Python’s multiprocessing package (default) or Open MPI [31, 32]. The inputs for one mesh element of each material in the calculation whose neutron flux is zero along with all of the mesh elements whose neutron flux is non-zero are added to either the queue in Multiprocessing mode or the list of inputs in OpenMPI mode for processing by the workers; either subprocesses or MPI processes. The results from the zero-flux runs are used to get place holder data for the rest of the zero-flux mesh elements with the corresponding material. The place holder data is essential for correct visualization of the data. Without the place holder data, the mesh elements whose flux is zero would contain a zero for all nuclides in the results database. Once the worker has completed a CINDER2008 run for a single mesh element, the worker writes the results to it’s own HDF5 database.

Once all of the transmutation calculations have been executed, all of the worker HDF5 databases are merged into one main HDF5 database. The place holder data of the mesh elements whose neutron flux is zero is then added to the master HDF5 database. Finally, a XDMF file is written to accompany the main HDF5 database. The XDMF file is used to point to the data in the HDF5 database without having to load the entire HDF5 database. The HDF5 database contains activity, activity density, mass, and decay heat for each nuclide in each mesh element along with the mass density, atom density, and volume of each mesh element. The XDMF file breaks down the information in the HDF5 database by part and information category for easier data viewing. The Activation module also includes some ParaView post-processing macros that allow the user to create custom datasets within ParaView like isotopic ratios and elemental concentrations.

## 2.3 Pre-Processing Procedure

In order to calculate the stable and radioactive isotopes produced by a nuclear detonation in an urban environment, the geometry of the city needs to be constructed and converted to a format conducive for particle transport with MCNP6.2.

The general building and terrain footprints of an urban environment can be gathered from OpenStreetMap directly or purchased in an importable CAD format from CADMAPPER [33, 34]. The CADMAPPER website provides a user interface to create 3D CAD models of the terrain, buildings, roads, parks, waterways, etc. for any user-selected region of the map. Once the user has selected a region of the map, a 3D CAD model can be generated and imported into the user's CAD program of choice. The data downloaded directly from OpenStreetMap has to be edited and converted before the user can import it into a CAD program. JOSM is an open source extensible editor for OpenStreetMap data, and within JOSM, the user can edit the OpenStreetMap data to delete certain features not necessary for valid representation of the urban environment; such as lines representing roads, subway tracks, park benches, trees etc. [35]. Once the OpenStreetMap data is cleaned up in JOSM, the user can then open the OpenStreetMap data in OSM2World to convert the data into a importable CAD file format [36]. Once the urban environment data is imported into a CAD program, the user must clean-up the model to ensure that there are no overlaps, interferences, or spline surfaces in the model and make sure the overall model is "water-tight."

Once the model is "water-tight" the user must create an unstructured mesh (UM) representation of the CAD model, and write the mesh as an Abaqus/CAE<sup>®</sup> input file. There are number of methods to generate the UM representation of the CAD model, but this paper will focus on the most prominent methods. Abaqus/CAE<sup>®</sup> is able to import the CAD model and generate a UM representation. Kulesza's UM tutorial using Abaqus/CAE<sup>®</sup> 6.12-1 provides a detailed procedure for generating the UM Abaqus/CAE<sup>®</sup> input file for MCNP6.2 [37]. SilverFur's Atilla4MC software is designed for UM generation specifically for particle transport with MCNP6 [38]. Atilla4MC allows the user to generate the UM representation of the CAD model also able to generate a UM representation of the CAD model and write the Abaqus/CAE<sup>®</sup> input file. Once the Abaqus/CAE<sup>®</sup> input file is generated, a MCNP6.2 calculation can be set up by following the procedure described in Martz's overview of the usage of UM in MCNP6.2, and using the material cards from the Material Processing Module described in Section 2.1 [39]. Figure 2 shows an high level overview of the pre-processing procedure.

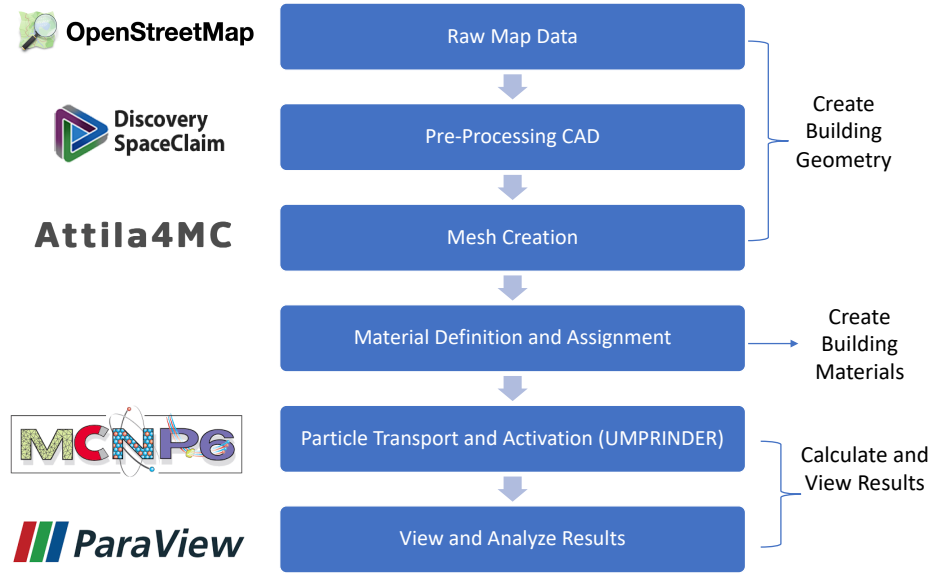
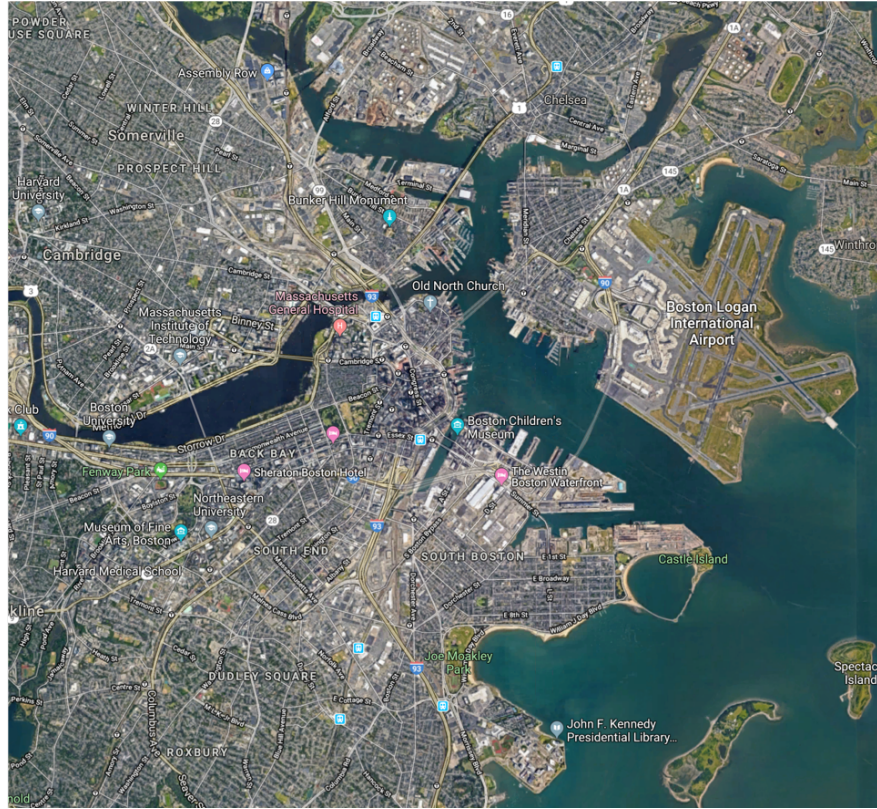


Figure 2: Overview of the Pre-Processing Procedure.

### 3 Results

The city of Boston is modeled in the Figure 3 and a 100 kT ground detonation is simulated using the process outlined in Sections 2.1, 2.2 and 2.3 at the source location shown in Figure 4. Northrop Source 8 is used as the neutron source in the MCNP6.2 calculation and the materials in the model are transmuted using the UMPRINDER code [40]. Figure 5 shows some of the isotope specific activities generated by neutron capture in stable isotopes in the city. Components such as the water and some of the building types, in the model that do not contain results for the nuclides of interest are not shown in Figure 5. Figure 6 shows isotopic ratios of some of the isotopes produced by neutron activation. The isotopes produced by neutron activation in the urban environment close to ground zero will likely be transported from the locations shown in the figures below due to a portion of them being swept up into the fireball, buildings collapsing, fires burning and lofting them into the atmosphere, etc. The results shown below can be used as a source term for fallout and fire modeling codes.



(a) Satellite Image of Boston, MA



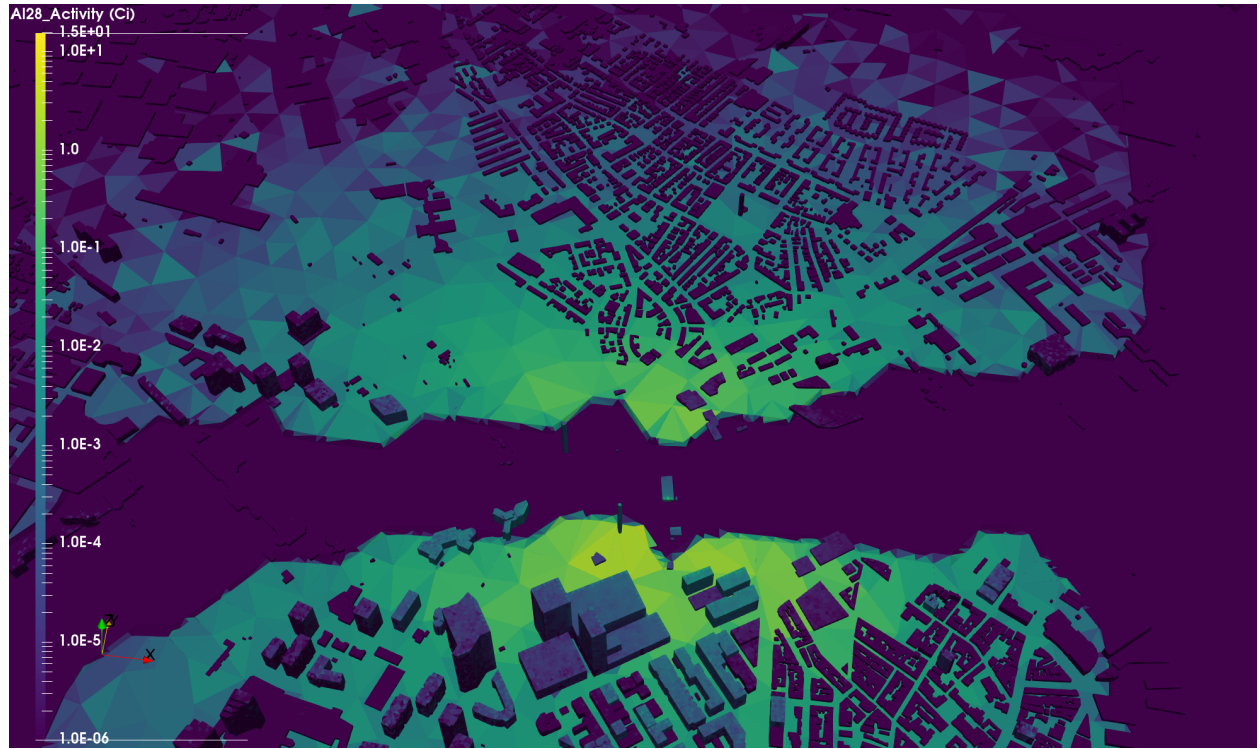
(b) CAD Model of Boston, MA

Figure 3: Overview of Boston, MA Model

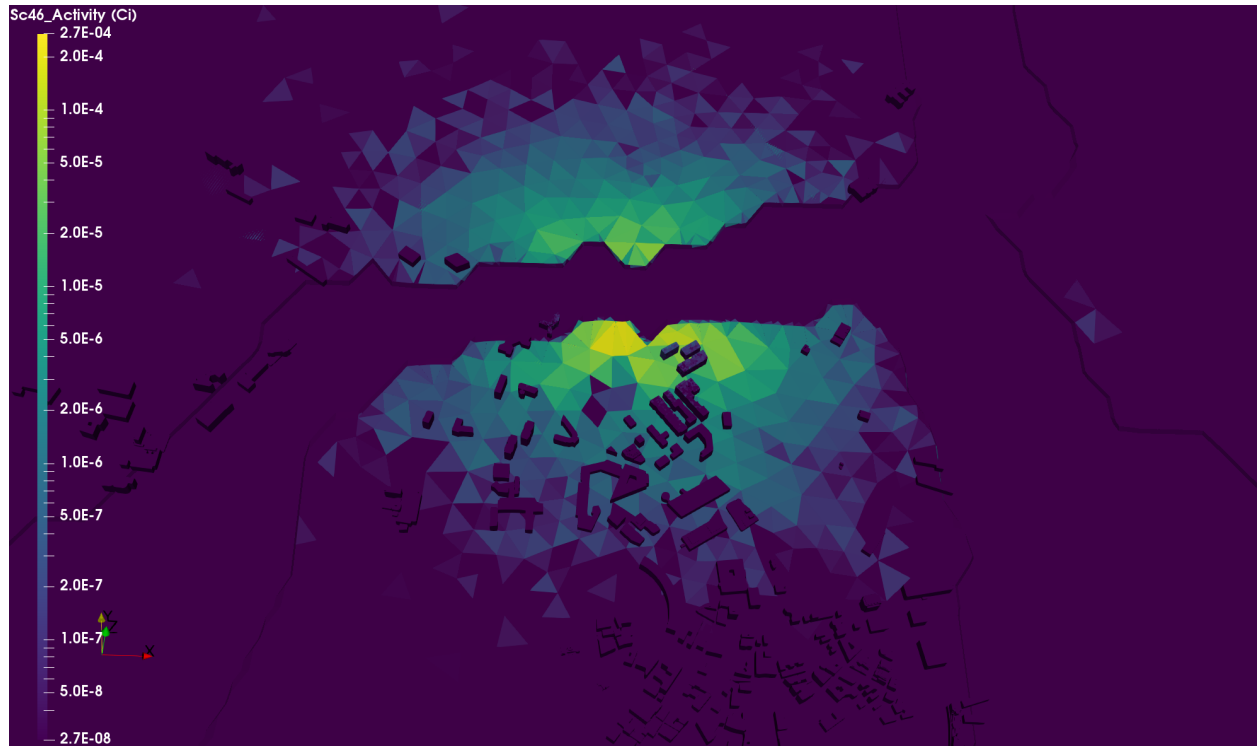


Figure 4: Overview of the Source Location



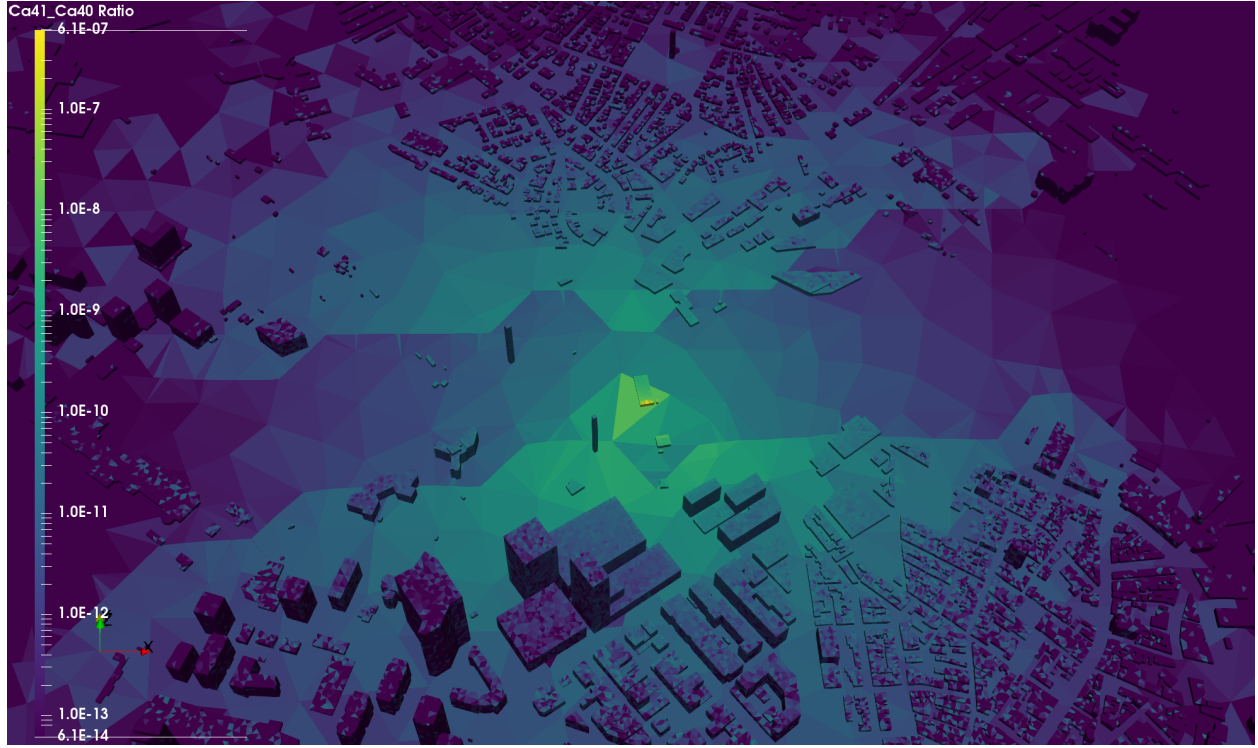


(a) Neutron activated  $^{28}\text{Al}$  activity (Ci)

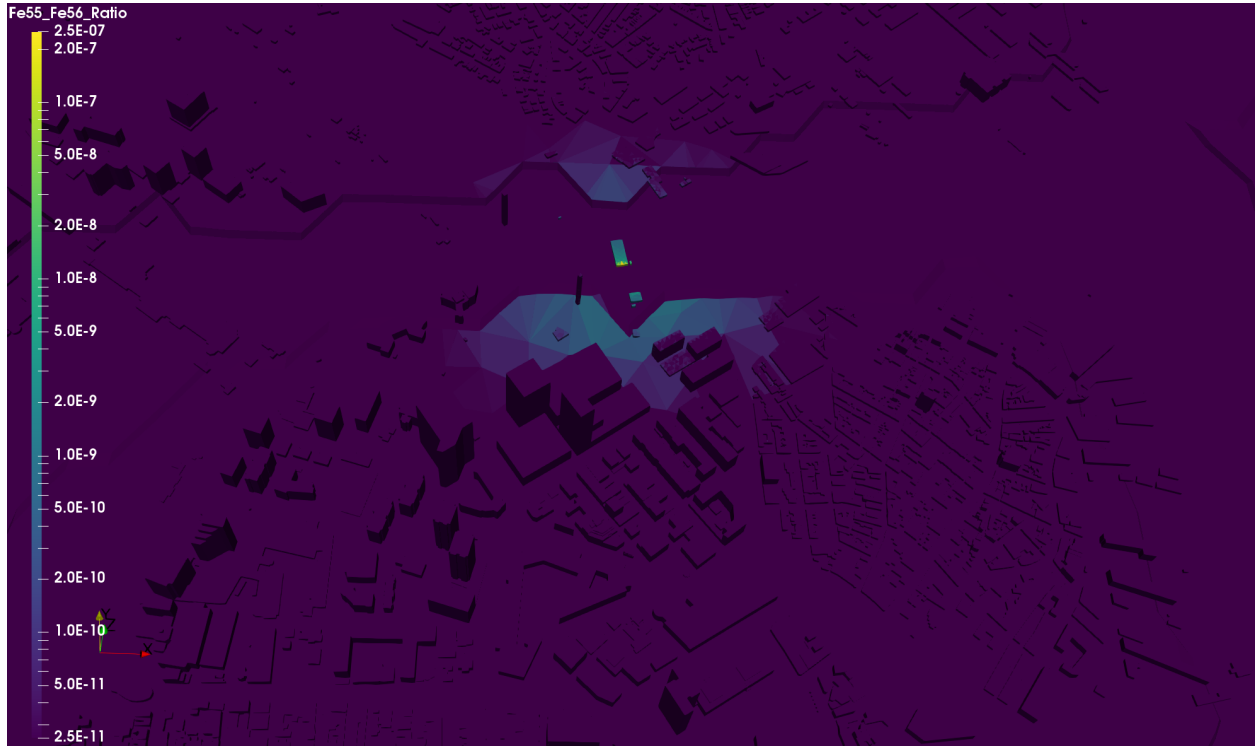


(b) Neutron activated  $^{46}\text{Sc}$  activity (Ci)

Figure 5: Neutron activated isotopic activity at 10 seconds post detonation



(a) Isotopic ratio for  $^{41}\text{Ca}/^{40}\text{Ca}$



(b) Isotopic ratio for  $^{55}\text{Fe}/^{56}\text{Fe}$

Figure 6: Isotopic ratios for products of neutron activation at 10 seconds post detonation



## 4 Summary

UMPRINDER is a new code that joins together the unstructured mesh capability of MCNP6.2 with the transmutation fidelity of CINDER2008 as apart of the AARE package to produce quantities of interest to the post detonation nuclear forensics and weapon effects communities. The city of Boston is modeled using the newly developed methodology of creating a unstructured mesh representation of a city based on the procedure described in Sections 2.1 & 2.3. The results from UMPRINDER calculating the neutron activated quantities from a 100 kT ground detonation demonstrated that isotopic specific quantities can be analyzed on the city mesh.

## References

- [1] NSSIPCS, “Planning guidance for response to a nuclear detonation,” FEMA, Tech. Rep., 2010.
- [2] D. B. Smith, W. F. Cannon, L. G. Woodruff, F. Solano, J. E. Kilburn, and D. L. Fey, “Geochemical and mineralogical data for soils of the conterminous united states,” U.S. Geological Survey Data Series 801, Tech. Rep., 2013.
- [3] E. Jones, T. Oliphant, P. Peterson *et al.*, “SciPy: Open source scientific tools for Python,” 2001–. [Online]. Available: <http://www.scipy.org/>
- [4] F. Kleemann, J. Lederer, P. Aschenbrenner, H. Rechberger, and J. Fellner, “A method for determining buildings’ material composition prior to demolition,” *Building Research & Information*, vol. 44, no. 1, pp. 51–62, 2016. [Online]. Available: <https://doi.org/10.1080/09613218.2014.979029>
- [5] F. Kleemann, J. Lederer, H. Rechberger, and J. Fellner, “GIS-based Analysis of Vienna’s Material Stock in Buildings,” *Journal of Industrial Ecology*, vol. 21, no. 2, pp. 368–380, 2017. [Online]. Available: <https://onlinelibrary.wiley.com/doi/abs/10.1111/jiec.12446>
- [6] M. Ueberschaar and V. S. Rotter, “Enabling the recycling of rare earth elements through product design and trend analyses of hard disk drives,” *Journal of Material Cycles and Waste Management*, vol. 17, no. 2, pp. 266–281, 2015. [Online]. Available: <https://doi.org/10.1007/s10163-014-0347-6>
- [7] M. Oguchi, S. Murakami, H. Sakanakura, A. Kida, and T. Kameya, “A preliminary categorization of end-of-life electrical and electronic equipment as secondary metal resources,” *Waste Management*, vol. 31, no. 9, pp. 2150 – 2160, 2011. [Online]. Available: <http://www.sciencedirect.com/science/article/pii/S0956053X11002510>
- [8] A. Muller, “The chemistry of the mobile phones Nokia Nuron 5230, Nokia 5130 and Sony Ericsson W595,” Geological Survey of Norway, techreport 2013.026, Jan. 2013.
- [9] J. Szalatkiewicz, “Metals content in printed circuit board waste,” *Polish Journal of Environmental Studies*, vol. 23, pp. 2365–9, 2014.
- [10] R. M. Jr., C. Gesh, R. Pagh, R. Rucker, and R. W. III, “Compendium of material composition data for radiation transport modeling,” PNNL, Tech. Rep. PNNL-15870 Rev. 1, Mar. 2011.
- [11] Y.-S. Chung, Y.-J. Chung, E.-S. Jeong, and S.-Y. Cho, “Determination of trace elements in airborne particulates by instrumental neutron activation analysis,” *Nuclear Engineering and Technology*, vol. 27, no. 2, pp. 234–247, 1995.
- [12] NIST, *Brick Clay*, National Institute of Standards and Technology Std. SRM 679, Jan. 1987.
- [13] J. Tejada, P. Grammer, A. Kappler, and H. Thorwarth, “Trace element concentrations in firewood and corresponding stove ashes,” *Energy and Fuels*, vol. 33, no. 3, pp. 2236–2247, 2019. [Online]. Available: <https://doi.org/10.1021/acs.energyfuels.8b03732>
- [14] S. Meier, “Elemental analysis of wood fuels,” Northeast States for Coordinated Air Use Management, Tech. Rep. NYSERDA Report 13-13, Jun. 2013.

- [15] A. Wyttenbach, V. Furrer, P. Schlegli, and L. Tobler, "Rare earth elements in soil and in soil-grown plants," *Plant and Soil*, vol. 199, no. 2, pp. 267–273, Feb 1998. [Online]. Available: <https://doi.org/10.1023/A:1004331826160>
- [16] N. J. Pearce, W. T. Perkins, J. A. Westgate, M. P. Gorton, S. E. Jackson, C. R. Neal, and S. P. Chenery, "A Compilation of New and Published Major and Trace Element Data for NIST SRM 610 and NIST SRM 612 Glass Reference Materials," *Journal of Geostandards and Geoanalysis*, vol. 21, no. 1, pp. 115–144, 1996.
- [17] D. Hickman, "Elemental analysis and the discrimination of sheet glass samples," *Forensic Science International*, vol. 23, no. 2, pp. 213 – 223, 1983. [Online]. Available: <http://www.sciencedirect.com/science/article/pii/0379073883901494>
- [18] E. Yilmaz, H. Baltas, E. Kırıs, I. Ustabas, U. Cevik, and A. El-Khayatt, "Gamma ray and neutron shielding properties of some concrete materials," *Annals of Nuclear Energy*, vol. 38, no. 10, pp. 2204 – 2212, 2011. [Online]. Available: <http://www.sciencedirect.com/science/article/pii/S0306454911002222>
- [19] R. K. Taggart, J. C. Hower, G. S. Dwyer, and H. Hsu-Kim, "Trends in the rare earth element content of u.s.-based coal combustion fly ashes," *Environmental Science & Technology*, vol. 50, no. 11, pp. 5919–5926, 06 2016. [Online]. Available: <https://doi.org/10.1021/acs.est.6b00085>
- [20] NIST. (2018, Jan.) Nist chemistry webbook, srđ 69. website. National Institute of Standards and Technology. Gaithersburg, MD.
- [21] H. H. Murray, "Chapter 2 structure and composition of the clay minerals and their physical and chemical properties," in *Applied Clay Mineralogy*, ser. Developments in Clay Science, H. H. Murray, Ed. Elsevier, 2006, vol. 2, pp. 7 – 31. [Online]. Available: <http://www.sciencedirect.com/science/article/pii/S1572435206020022>
- [22] ScienceDirect. (2019, Sep.) Dolomite. website. ScienceDirect. [Online]. Available: <https://www.sciencedirect.com/topics/engineering/dolomite>
- [23] C. E. Weir and E. R. Lippincott, "Infrared studies of aragonite, calcite, and vaterite type structures in the borates, carbonates, and nitrates," *Journal of Research of the National Bureau of Standards – A. Physics and Chemistry*, vol. 65A, no. 3, pp. 173–83, Jan. 1961.
- [24] R. T. Wilkin and H. L. Barnes, "Solubility and stability of zeolites in aqueous solution: I. analcime, na-, and k-clinoptilolite," *American Mineralogist*, vol. 83, pp. 746 – 761, 1998.
- [25] A. Augustyn, P. Bauer, B. Duignan, A. Eldridge, E. Gregersen, A. McKenna, M. Petruzzello, J. P. Rafferty, M. Ray, K. Rogers, A. Tikkanen, J. Wallenfeldt, A. Zeidan, and A. Zelazko. (2019, Sep.) Hornblende. website. Encyclopedia Britannica. [Online]. Available: <https://www.britannica.com/science/hornblende>
- [26] Y. Chen and U. Fischer, "Rigorous mcnp based shutdown dose rate calculations: computational scheme, verification calculations and application to iter," *Fusion Engineering and Design*, vol. 63-64, pp. 107 – 114, 2002. [Online]. Available: <http://www.sciencedirect.com/science/article/pii/S0920379602001448>
- [27] J. A. Clarke and E. R. Mark, "Enhancements to the extensible data model and format (xdmf)," in *HPCMP Users Group Conference*. IEEE Computer Society, 2007.

- [28] M. Folk, G. Herber, Q. Koziol, E. Pourmal, and D. Robinson, “An Overview of the HDF5 Technology Suite and its Applications,” in *ICDT: The International Conference on Database Theory*, ser. ICPS - International Conference Proceedings Series, J. Stoyanovich, Ed., ICDT. ACM New York, 2011.
- [29] H. Childs, E. Brugger, B. Whitlock, J. Meredith, S. Ahern, D. Pugmire, K. Biagas, M. Miller, C. Harrison, G. H. Weber, H. Krishnan, T. Fogal, A. Sanderson, C. Garth, E. W. Bethel, D. Camp, O. Rübel, M. Durant, J. M. Favre, and P. Navrátil, “VisIt: An End-User Tool For Visualizing and Analyzing Very Large Data,” in *High Performance Visualization—Enabling Extreme-Scale Scientific Insight*, Oct 2012, pp. 357–372.
- [30] J. Ahrens, B. Geveci, and C. Law, “Paraview: An end-user tool for large data visualization,” LANL, Tech. Rep. LA-UR-03-1560, 2003.
- [31] G. van Rossum. (2019) multiprocessing – process-based parallelism. website. Python. [Online]. Available: <https://docs.python.org/3.6/library/multiprocessing.html>
- [32] R. L. Graham, G. M. Shipman, B. W. Barrett, R. H. Castain, G. Bosilca, and A. Lumsdaine, “Open mpi: A high-performance, heterogeneous mpi,” in *2006 IEEE International Conference on Cluster Computing*, Sep. 2006, pp. 1–9.
- [33] M. Haklay and P. Weber, “Openstreetmap: User-generated street maps,” *IEEE Pervasive Computing*, vol. 7, no. 4, pp. 12–18, 2008.
- [34] Cadmapper, “CADMAPPER,” website, Cadmapper, LLC, Apr. 2018. [Online]. Available: <https://cadmapper.com>
- [35] I. Scholz and D. Stocker. (2019, Jul.) JOSM. website. GNU General Public License. [Online]. Available: <https://josm.openstreetmap.de>
- [36] T. Knerr. (2019, Jun.) OSM2World. website. GNU Lesser General Public License. [Online]. Available: <http://osm2world.org>
- [37] J. A. Kulesza and R. L. Martz, “MCNP6 Unstructured Mesh Tutorial Using Abaqus/CAE 6.12-1,” LANL, Tech. Rep. LA-UR-15-25143, 2015.
- [38] G. Failla, *Atilla Radiation Transport Software Tutorial: Transmutation/Activation*, Transpire, Inc., 2012.
- [39] R. L. Martz, “The MCNP6 Book on Unstructured Mesh Geometry: User’s Guide for MCNP6.2,” LANL, Tech. Rep. LA-UR-17-22442, Mar. 2017.
- [40] J. A. Northrop, Ed., *Handbook of Nuclear Weapon Effects*. Defense Threat Reduction Agency, 1996.